VALIDATION AND APPLICATION OF A FINITE ELEMENT PEDESTRIAN HUMANOID MODEL FOR USE IN PEDESTRIAN ACCIDENT SIMULATIONS

Mark Howard, Alan Thomas, Werner Koch
Ford Forschungszentrum Aachen GmbH

James Watson, Roger Hardy
Cranfield Impact Centre Ltd

ABSTRACT

Pedestrian protection is an important societal issue and over the last 15 years two main research approaches have developed to address this issue; the proposed European draft directive and real world pedestrian accident simulation. In this study the latter approach was used in order to study the complex interaction between pedestrians and vehicles during real world pedestrian accidents.

A comprehensive research programme has been undertaken over the last four years. This paper describes two of the main projects within this programme: the creation and development of finite element models of pedestrian humanoids and the application of these models in real world pedestrian accident simulations. It addresses whether a simplified finite element model of a pedestrian may be used in detailed pedestrian accident simulations to gain a better understanding of the pedestrian and vehicle interaction and presents some initial results regarding this interaction.

KEYWORDS

Pedestrians, Finite Element Models, Injury Mechanisms, Safety, Validation

PEDESTRIAN PROTECTION is an important research field that concerns the societal issue of pedestrian safety. Accident statistics such as those shown in Figure 1 indicate that in overall terms (although not necessarily in each age group for instance) pedestrian fatalities and injury levels are falling but the figures are still too high.

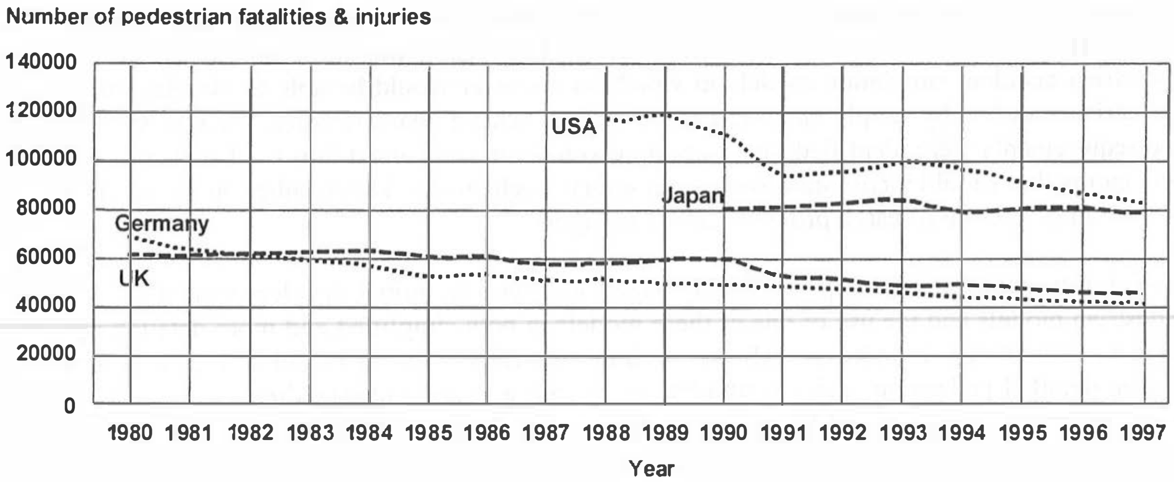

Figure 1 Trends in pedestrian fatalities and injuries in various countries [OECD, 1998-1]

Pedestrians form one of the major road user groups and it is therefore useful to consider the proportion of pedestrian fatalities compared to other road user groups, as shown in Figure 2.

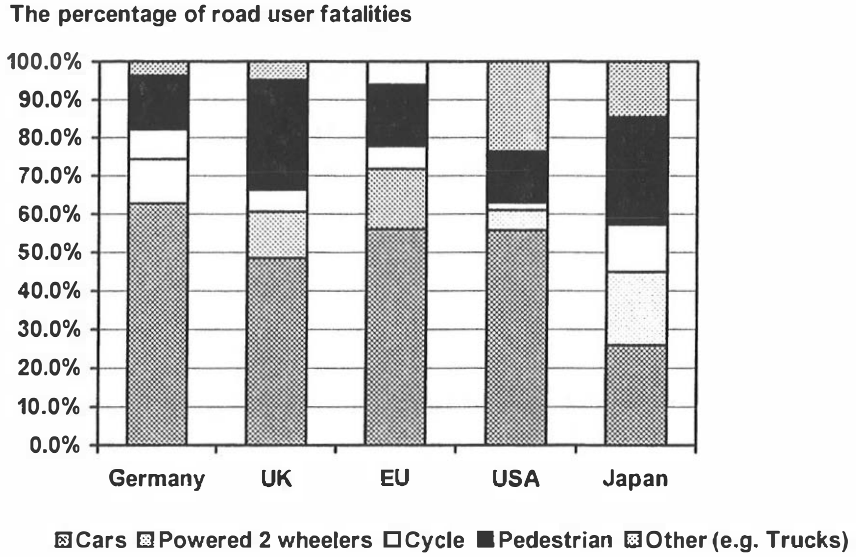

Figure 2 The breakdown of total road user fatalities by road user group in 1995 [OECD, 1998-2]

In the EU as a whole, pedestrians form the second largest road user fatality group and this is also reflected in the UK and Germany but not in the USA (e.g. because car usage is higher in the USA). In Japan, the pedestrian group is the largest fatality group.

It is the responsibility of society and not one stakeholder (e.g. vehicle manufacturers) to implement pedestrian protection solutions. Each stakeholder has a limited area in which they have a primary influence and can contribute to solutions (e.g. governments can influence public transport infrastructures). This paper concentrates on the research efforts of one stakeholder to understand the real nature of pedestrian accidents by using a combination of experimental testing and finite element modelling to create and analyse pedestrian accident scenarios. The purpose of such an approach is to achieve an improved understanding of real world pedestrian accidents. Other types of approach have been previously described and published within a conceptual framework [Howard et al., 1998-2, Howard and Thomas, 1998-1, Howard and Thomas, 1999].

Having tried other research approaches, in 1996, the Ford Forschungszentrum Aachen GmbH (FFA) offered a future vision for pedestrian safety. This vision was to be able to create real world pedestrian accident simulation models in which an engineer would be able to simulate any type of pedestrian accident by simply entering pedestrian and vehicle characteristics. To achieve this vision, two requirements were identified: more accurate vehicle models and a family of scaleable pedestrian humanoids that should incorporate significant injury mechanisms. This resulted in the creation of the pedestrian protection research program shown in Figure 3.

Within the context of this program this paper describes the initial development of the humanoid pedestrian models and the use of one of these models in both simplified and more detailed pedestrian accident simulations. It addresses whether a simplified finite element model of a pedestrian may be used in detailed pedestrian accident simulations to gain a better understanding of the pedestrian and vehicle interaction and presents some initial results regarding this interaction.

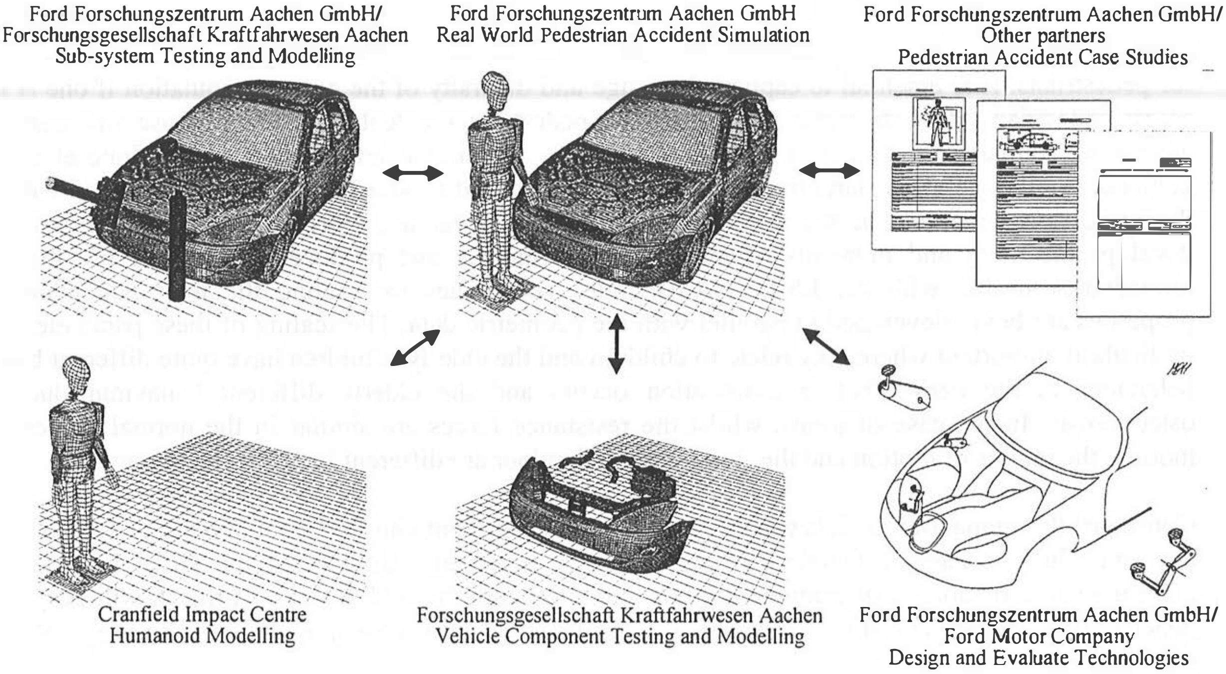

Figure 3 The FFA pedestrian protection research program [Hardy et al., 2000]

FINITE ELEMENT PEDESTRIAN HUMANOID MODELS

FORMULATION The formulation of the humanoid model that was originally based on dummy datasets is gradually being upgraded to have a flexible and fully deformable limb formulation. The construction is based on a finite element representation that can be employed with vehicle finite element models to allow greater interaction between the two models than can be achieved by a rigid element formulation with contact stiffness.

The aim in the humanoid modelling was to achieve a human like representation with biofidelic properties, yet avoiding a detailed finite element construction. Detailed models would require considerable computer processing time and prevent use of the models for the rapid assessment of pedestrian protection technologies. The modelling approach was first to identify the primary injury locations, which would need greater attention as they represented the most frequent and more severe injury mechanisms [MacLaughlin et al., 1987, Ashton, 1978, Langwieder et al., 1980]. Secondly, to construct finite element models of these regions and develop them to maturity.

The humanoid mathematical models were constructed to examine overall kinematics and assess the likely occurrence of injury mechanisms (e.g. bone fracture, ligament rupture and soft tissue injuries). For these purposes and the detail model constraints, the bones of the leg, for example, where modelled as a series of beams to represent the femur and tibia - the patella and fibula were omitted for lateral impacts as recommended by Bermond et al. [1993]. The beams were formulated to give elastic deformation up to the point where bone fracture would occur. Solid elements were attached to the beams at coincident nodes, allowing loads generated in the solids due to compression to pass directly into the beams. At the knee joint three rotational and three translational springs were utilised to represent the full ranges of motion present in a human knee. Similarly, in the neck model, a formulation with seven rigid cervical vertebrae and a six degree of freedom joint between each was implemented in LS-DYNA-3D, based on the Global model developed by de Jager [1996].

Further details of the exact construction employed in the body models and the material properties used to describe them have been described in previous publications [Howard et al., 1998, Hardy et al., 2000] - that also include details of the validation activities carried out on individual body regions.

The development of a 50th percentile finite element humanoid model is only part of the whole story for pedestrians. It is essential to capture the range and diversity of the human population if one is to assess pedestrian safety strategies and reconstruct pedestrian accidents. For this purpose a process of generating Humanoid models has been developed. To aid further development of the finite element humanoids, all generation starts from a 'reference model' that is adjusted for size and shape based on the regression equations in the GEBOD program [Cheng et al., 1991]. The generation process develops the mass and moments of inertia for the models and produces a keyword file that is immediately usable with the LS-DYNA3D code. Techniques for scaling the joint and material properties are being developed in parallel with the geometric data. The scaling of these parameters is particularly important where they relate to children and the elderly. Children have quite different bone behaviour in the period before ossification occurs and the elderly different behaviour due to osteoporosis. In the case of joints, whilst the resistance forces are similar in the normal ranges of motion, the ranges of motion and the 'joint-stop' behaviour are different between the two groups.

Consequently, humanoid models can be generated that represent children from 3 years to 15 years of age and adults - male or female - from 5th to 95th percentile. Updates of the GEBOD program anthropometric database, for example with the completion of the SAE's Caesar Project, will keep the generated humanoids current with the sizes and shapes of the current population. The range of the models generated is illustrated in Figure 4.

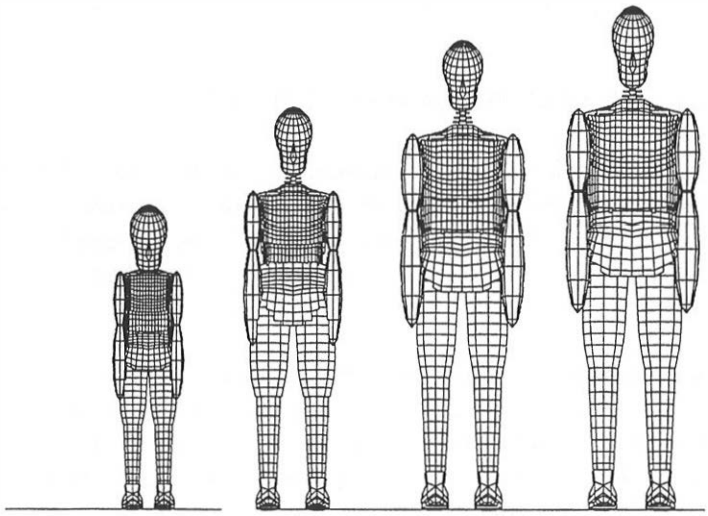

Figure 4 Generated 6 year, 5th female and 50th and 95th male humanoids

USE OF THE MODELS Simulations and parametric studies in previous published work [Howard et al., 1998, Hardy et al., 2000] have indicated that two parameters, vehicle speed and bumper (car front) height, were the cause of the greatest variation in simulation results and predicted injury mechanisms. Overall body kinematics were greatly influenced by the standing position (stance) of the humanoid. With the legs together and the humanoid sideways to the car, the humanoid generally fell sideways with little rotation about his vertical axis. However, with a fore and aft separation of the legs the humanoid rotated about his vertical axis to finish face down or face up on the car.

In a further parametric study when vehicle impact speeds were 25km/h or above, the effect of changes in biomechanical properties (e.g. Young's Modulus of bone, knee rotational and shear stiffness and strength) were investigated. Whilst these type of biomechanical parameters (derived from cadaver tests) often have large variations in values between nominally identical studies by different researchers, it was established that the variation in numerical simulation results were limited to no more than 20%. Small changes in injury mechanisms were predicted.

HUMANOID VALIDATION

INITIAL CONDITIONS To validate the finite element model of the humanoid it was necessary to compare its response with data from impacts with pedestrians. Real world comparisons would be ideal but the variability and element of doubt over some key information involved in using real world data dictated against this method. Instead data from staged pedestrian impacts using cadavers as pedestrian substitutes were used. The particular data selected was reported by Ishikawa et al. [1993] and has subsequently been used by other researchers [Akiyama et al., 1999]. For the validation of the humanoid its responses were compared to the results from two of the tests. These tests were chosen since they covered a wide separation in impact speeds and vehicle geometry. Table 1 gives details of the vehicle geometry and cadaver data.

Test	Velocity (km/h)	Car Shape	Age (years)	Sex	Mass (kg)	Height (m)
T1	25	C1	54	m	75	1.80
T9	39	C2	68	m	88	1.75

Table 1 Set-up for cadaver tests

Full details of the vehicle shapes and the contact stiffness of the vehicle components used in the tests are given by Ishikawa [1993] and are summarised in Table 2. Here, the actual values of bumper and bonnet height are shown after adjustment for changes in vehicle attitude as a consequence of the breaking effect.

Car Shape	Bumper lead (m)	Bumper height (m)	Bonnet height (m)	Bumper stiffness (kN/m)	Bonnet stiffness (kN/m)
C1	0.22	0.38	0.73	2000	2000
C2	0.20	0.39	0.72	2000	2000

Table 2 Vehicle shape and stiffness

The bumper, bonnet and windscreen geometry of the car were represented by separate rigid shell element parts linked back to the centre of gravity of the vehicle. The bumper and bonnet links incorporated springs representing the contact stiffness of the vehicle parts.

The initial simulation configurations with the different car bodies are shown in Figures 5 and 6 with the humanoid model, which is positioned in a walking stance with the left arm angled across the lower torso. A 10ms delay was allowed before the vehicle hit the humanoid to allow the humanoid to reach an equilibrium state with the ground. The friction coefficient between the ground and the humanoid was set at 0.67 and the friction coefficient with the vehicle was set as 0.25.

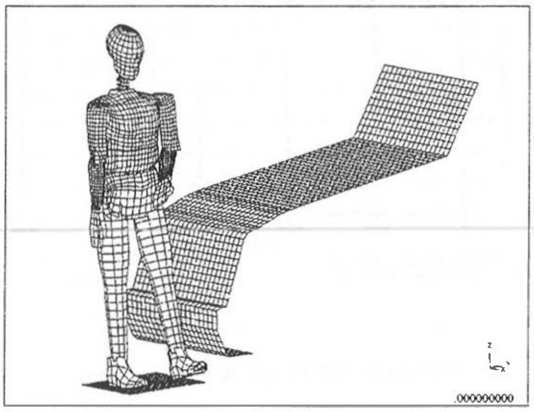

Figure 5 T1 set-up

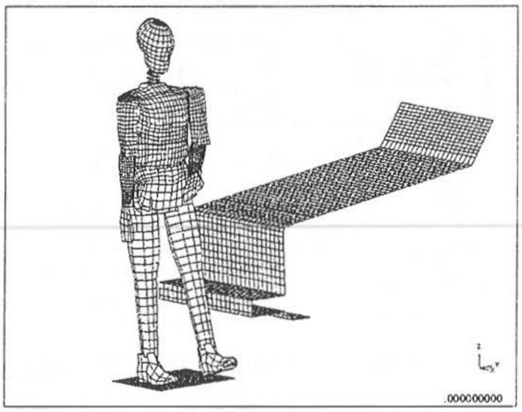

Figure 6 T9 set-up

The 50th percentile humanoid model described earlier was used as the basis for the programme of validation. However, the lumbar spine and pelvis contact stiffnesses were adjusted. These changes were instigated to align the formulation of the model more closely with the data in the mathematical model developed by Ishikawa and used to predict the same response as the cadaver tests. In addition, the impacted hand of the humanoid was positioned across the pelvis to prevent it interfering with the kinematics.

In initial simulations, the humanoid did not wrap around the front of the car, instead it was pushed away horizontally and vertically, rotating in the air and only making contact again just prior to head impact. By including a measure of hysteresis in the contacts with the bonnet, to represent energy absorption, this situation was corrected.

RESULTS Validation of the humanoid model was conducted on two levels; body segment trajectories and measured parameters (head resultant velocity). Body segment trajectories were obtained from target markers positioned on the head, pelvis, knee and foot during the cadaver tests. The trajectories from the humanoid model were compared against the measured trajectories. The comparisons are shown in Figure 7 for both the test configurations. For the T1 simulation the cadaver results have been normalised to match the height of the humanoid, but in the T9 simulation no adjustment was necessary.

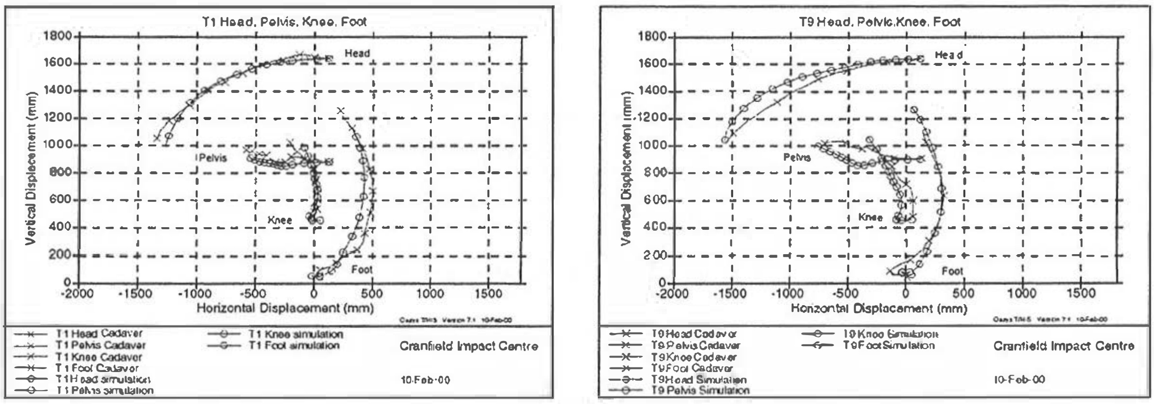

Figure 7 T1 and T9 Trajectories

The parameters from the humanoid model were compared against the measured parameters. The comparisons are shown in Figure 8 for the test T1 and test T9 configuration and Figures 9 - 11 for T9.

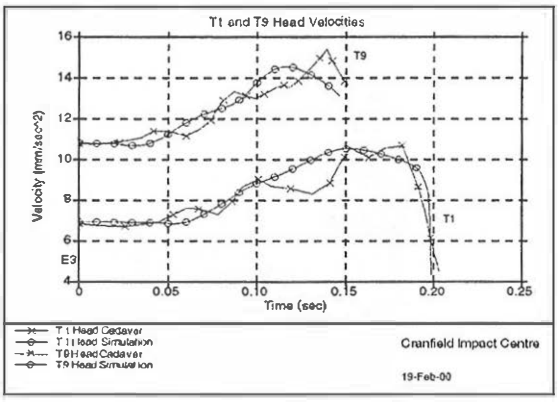

Figure 8 T1 and T9 Head Velocities

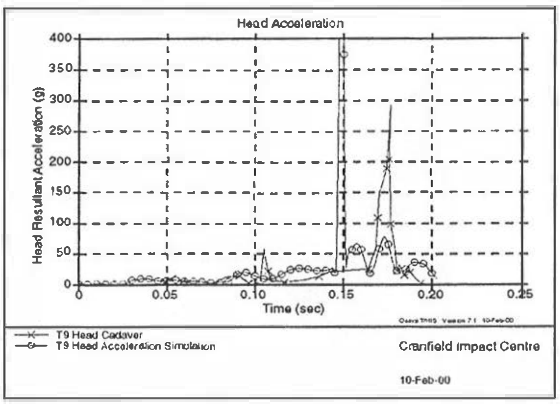

Figure 9 T9 Head Accelerations

DISCUSSION The trajectories of the humanoid model show very good correlation with the cadaver experiments for all body segments in the test T1 and T9 configurations. Similarly there was good correlation with the resultant head velocities across both test configurations.

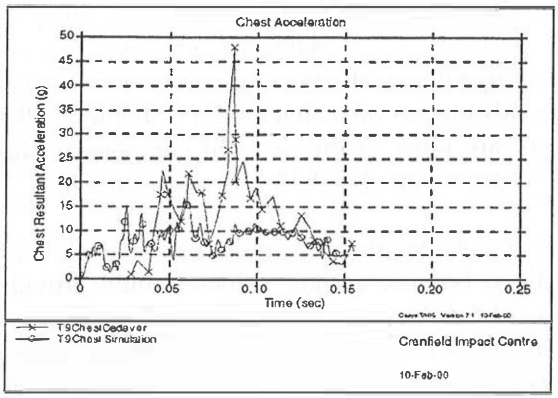

Figure 10 Chest Accelerations

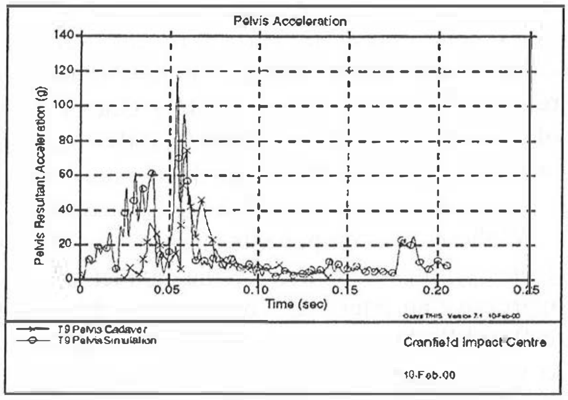

Figure 11 Pelvis Accelerations

Correlation of the accelerations in the test T9 configuration (accelerations not measured in test T1) was not as good as for trajectories and head velocities. Head accelerations, that are dependant on contact stiffness, were similar in wave form prior to head impact and impact was slightly early. The average chest acceleration levels were similar and the wave form prior to chest impact was similar but the simulation did not exhibit the same high contact levels. This difference is likely to result from a variance in the modes of contact with the bonnet of the car between the cadaver arm and the humanoid arm. Pelvis acceleration levels and timing were quite similar.

In the test T9 configuration the knee and foot trajectories were particularly pleasing since Ishikawa [1993] and Yoshida et al. [1998] noted that their simulation models were unable to predict leg trajectories at higher impact severities and ascribed this to the inability of their models to predict damage/injuries. The humanoid model has these capabilities and predicted lower leg fracture and knee damage, thus giving good trajectories. Nevertheless, whilst the knee and foot trajectories are better correlated, that for the knee still exhibited an early horizontal displacement. The exact location of the injuries is clearly important in order to predict the exact trajectories of the knee and foot. For this purpose it would be beneficial to know the precise point of impact of the bumper to the leg of the cadaver.

It may be concluded that to comprehensively predict the outcome of staged cadaver tests, it is not only important that the overall height of the subject be known but also the individual limb lengths, particularly in the case of the legs. In this way the interaction of the exact geometry of the car with specific anatomical features can be ensured. More exacting correlation of tests and computer predictions would then be possible.

SUMMARY The humanoid model has shown very good validation in terms of trajectories for the head, pelvis, knee and ankle against the trajectories of the cadaver tests. The head velocity has also shown very good validation, with the humanoid model accurately predicting the time of impact between the head and bonnet. The validation has been conducted up to velocities of 39km/h, which makes the humanoid model suitable for assessing many real world injury mechanisms, unlike the proposed legislative sub-system impactors that assess only a few. The humanoid model also has the advantage of being able to assess the influence of initial injury mechanisms on subsequent injury mechanisms and trajectories.

SIMPLIFIED PEDESTRIAN ACCIDENT SIMULATION MODELS

VEHICLE SET-UP The simplified vehicle model uses rigid body panels to represent the outer geometry of the bumper, bonnet and windscreen that are linked back to the centre of gravity of the vehicle by rigid links, in the case of the bonnet and windscreen and via a spring for the bumper. The mass and inertial properties of the vehicle are defined at the centre of gravity. The contact characteristics of the vehicle parts were derived from dynamic tests on components (similar to those reported by Suthurst et al. [1985]). One of the major advantages of such a model is that the CPU time of the model is reduced significantly, because there are none of the detailed components that are behind the bumper and under the bonnet. Run time is approximately 2 CPU hrs on a Sun Ultra.

Without any components such as the bumper core or the engine block modelled beneath the outer geometry the deflection of the bonnet is very critical, because a rigid vehicle would provide too aggressive an interface. To overcome this problem LS-DYNA contact type 21 (Rigid Body One Way to Rigid Body) was used which allows the user to specify a load curve between humanoid body parts to vehicle components. The load curves were derived from impact tests on a similar size vehicle. Thus, although the vehicle model was unable to locally deform due to any impact with the humanoid, the contact definitions allow for a representation of mutual interaction. An initial configuration of the vehicle and humanoid is shown in Figure 12.

To model the deceleration of the vehicle a spring was attached from the centre of gravity of the vehicle to a fixed point in space. This spring had a constant force level that was calculated from the mass of the vehicle to provide the necessary deceleration for the vehicle. The vehicle was not prescribed a velocity profile, but an initial velocity, which allowed it to freely interact with the humanoid. The spring and the vehicle components are all constrained to move in the direction of vehicle travel only. The brake dive of the vehicle was modelled by lowering the vehicle by 70mm.

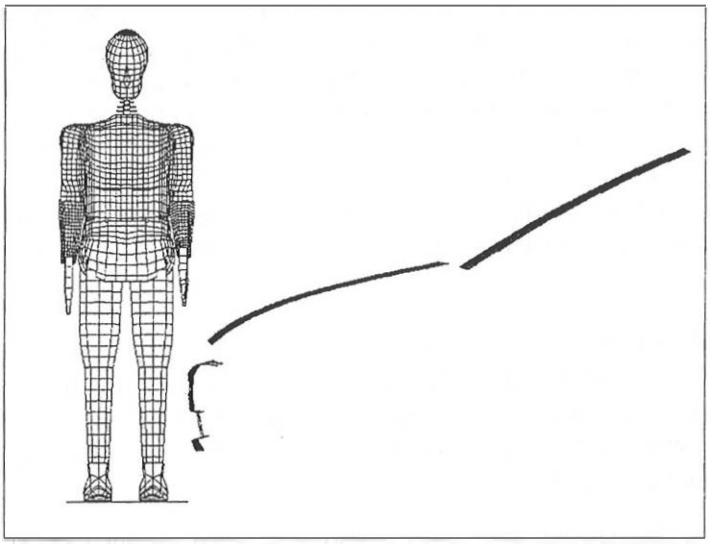

Figure 12 Vehicle and humanoid set-up

PARAMETRIC SIMULATIONS A series of six simulations were conducted to investigate the influence of vehicle parameters and for later comparison with a more detailed pedestrian accident model. These are shown in Table 3. Simulations were conducted for impacts at the centreline of the vehicle (Y0), since the simplified vehicle geometry represents only this region.

Simulation	Vehicle set-up
B07	25km/h, no brake dive, no deceleration
B03	25km/h, no brake dive, deceleration
B11	25km/h, brake dive, deceleration
B05	40km/h, no brake dive, no deceleration
B01	40km/h, no brake dive, deceleration
B09	40km/h, brake dive, deceleration

Table 3 Simulation set-up

RESULTS The kinematics for the six simplified simulations are shown in Figures 13 and 14. They show some of the key features from a pedestrian accident, such as the bending and shearing of the human knee and the articulation of the torso. The 40km/h runs were simulated to 200ms, the output was at every 10ms, but only 40, 70, 100 and 130ms are shown here. Similarly, at 25km/h the plots are shown at 50, 100,150 and 200 ms. Tabulated results are given in Table 4.

Simulation	Pelvis to bonnet (ms)	Left upper arm to bonnet (ms)	Head to bonnet/windscreen (ms)
B07	70	175	185
B03	No contact	178	190
B11	107	202	211
B05	40	118	126
B01	42	114	127
B09	54	93	144

Table 4 Contact times

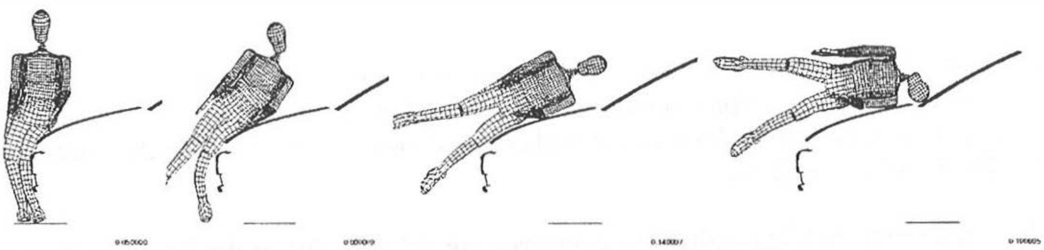

25km/h without deceleration or brake dive

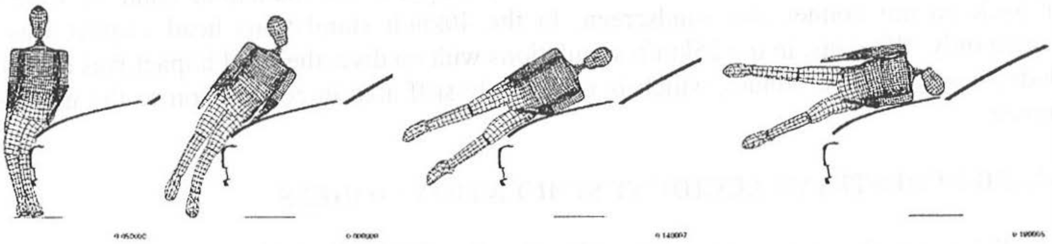

25km/h with deceleration, but no brake dive

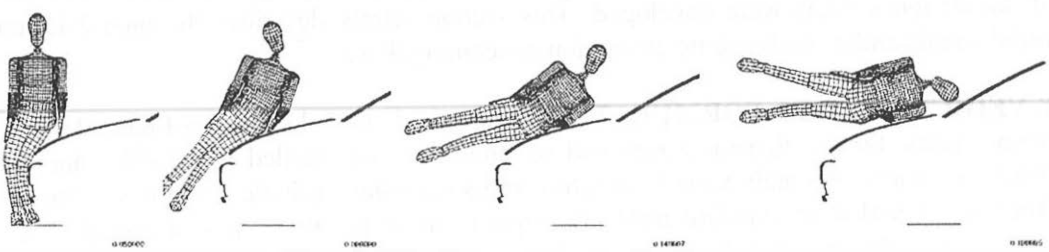

25km/h with deceleration and brake dive

Figure 13 Humanoid kinematics from 25km/h simulations

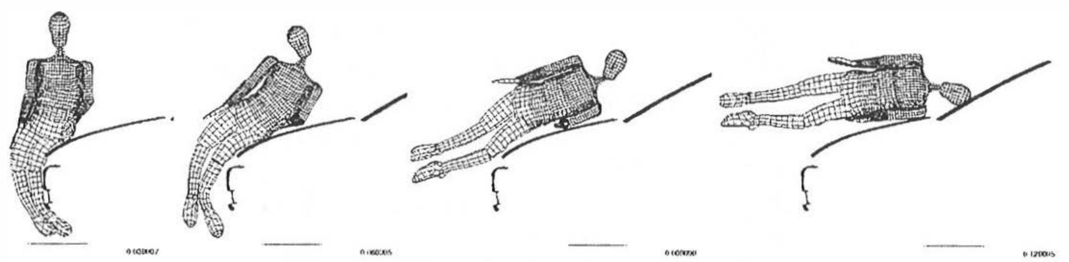

40km/h without deceleration or brake dive

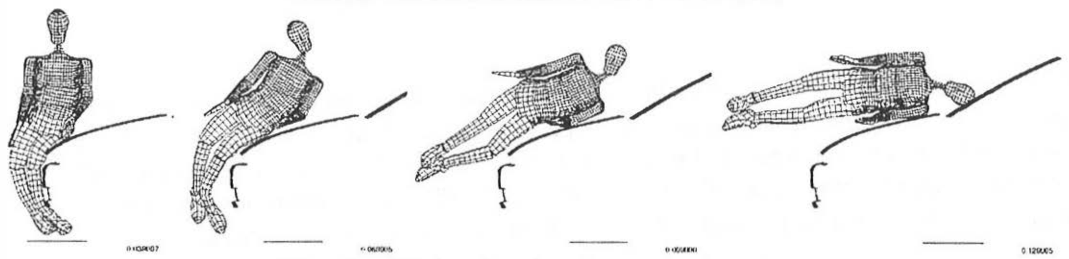

40km/h with deceleration, but no brake dive

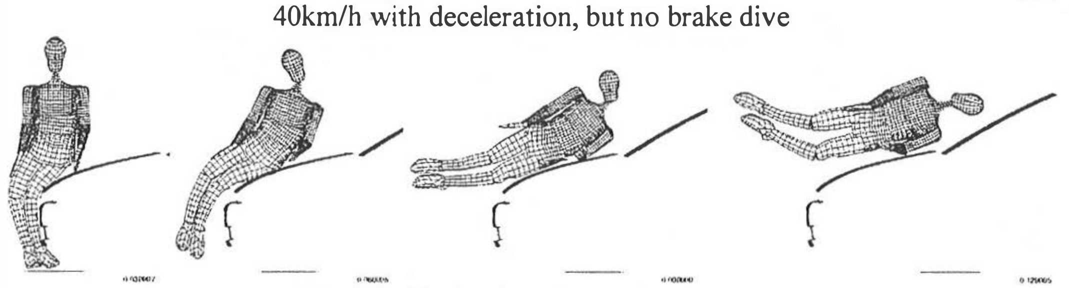

40km/h with deceleration and brake dive

Figure 14 Humanoid kinematics from 40km/h simulations

DISCUSSION The humanoid kinematics and all body segment contact times were very similar in the baseline and the 1g deceleration simulations (25 and 40 km/h). The difference in vehicle travel over a 200ms period was only 0.196m in the higher speed simulation - a relatively small distance compared to the total travel of 2.2m.

In all the simulations with brake dive the contacts were delayed, due to the lower position of the vehicle relative to the humanoid. In addition, at both speeds the humanoid contacts were located further back on the bonnet and windscreen. In the 40km/h simulations head contact was on the windscreen only. Whereas, in the 25km/h simulations with no dive, the head impact was at the base of the windscreen/top of the bonnet, which is a relatively stiff area in comparison to the middle of the windscreen.

DETAILED PEDESTRIAN ACCIDENT SIMULATION MODELS

In parallel to the development of the humanoid models a detailed vehicle model and pedestrian accident simulation models were developed. This section briefly describes the model formulation, some initial results and provides some discussion concerning these.

THE VEHICLE MODEL FORMULATION The vehicle model shown in Figure 15 consists of three distinct parts. Firstly, there is a rear end structure that is modelled in a rigid material with a coarse mesh. Secondly, the main vehicle structure and some minor vehicle components are modelled with a finer mesh and have standard material properties used in other types of model (e.g. frontal crash models). Finally, the more important vehicle components for pedestrian impact conditions are defined with material properties determined by a systematic testing and modelling methodology to characterise their behaviour under pedestrian impact energy levels. This methodology is based on the concept of removing vehicle components from a vehicle; experimentally impact testing them under pedestrian impact conditions and then using these results to validate finite element models of these components. Finally, the vehicle components have been incorporated into the detailed vehicle model.

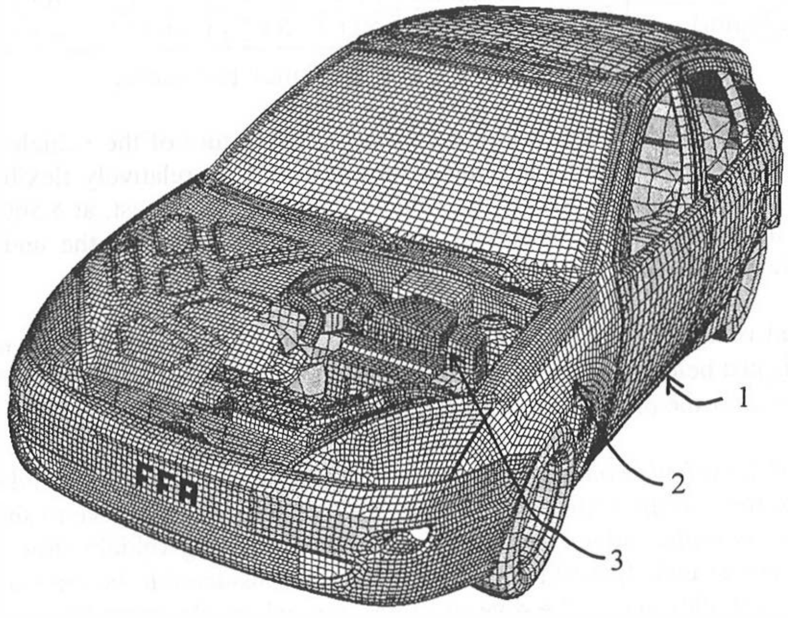

Figure 15 The detailed vehicle model

An example of the vehicle headlamp component validation test and the results is shown in Figure 16. More details regarding the systematic testing and modelling procedure and the vehicle components validated have been previously published [Howard et al., 2000, Philipps and Howard, 1999].

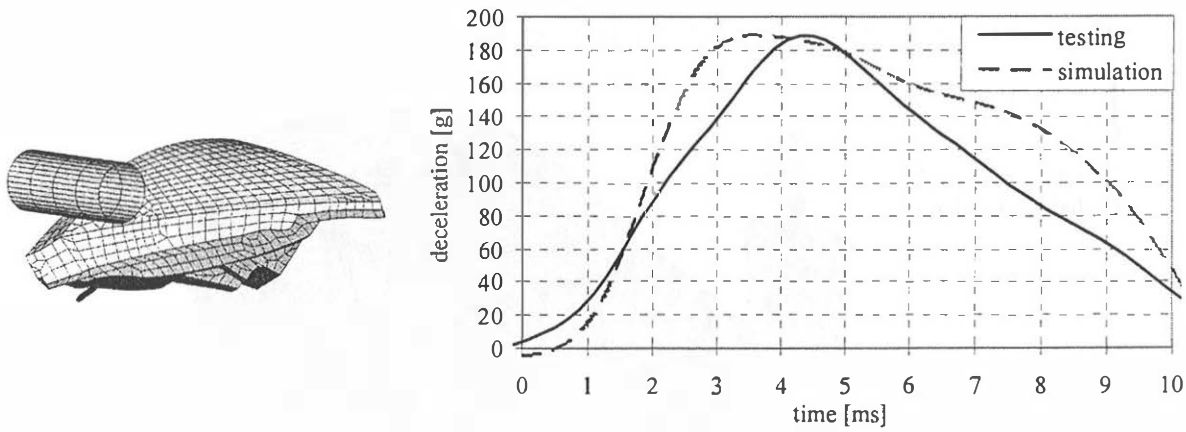

Figure 16 The headlamp component test procedure model and validation against experimental results

PEDESTRIAN ACCIDENT SIMULATION METHODOLOGY There were a total of seven boundary conditions considered; four of these were varied and three fixed. The vehicle impact location (Y0 and Y500), vehicle velocity (40km/h and 25 km/h), vehicle deceleration (1g and none), and vehicle brake dive (70mm and none) were varied whilst the type of vehicle (C class), the type of pedestrian humanoid (50th percentile male) and the pedestrian stance (side on with both legs together) were fixed. The simulation test matrix is shown in Table 5.

Vehicle velocity (km/h)	25						40					
Impact location (mm)	Y0			Y500			Y0			Y500		
Simulation run	B03	B07	B11	B04	B08	B12	B01	B05	B09	B02	B06	B10
Deceleration (1g)	YES	NO	YES	YES	NO	YES	YES	NO	YES	YES	NO	YES
Brake dive (70mm)	NO	NO	YES	NO	NO	YES	NO	NO	YES	NO	NO	YES

Table 5 The simulation test matrix

Two *impact locations* were chosen according to the nature of the vehicle shape and structure. At the vehicle centreline the initial leg impacts are low and the relatively flexible underlying beam and the bumper assembly inertia control the vehicle stiffness. In contrast, at Y500, the initial leg contacts are higher; the vehicle front is curved rearward in plan view and the underlying structure stiffer because of the longitudinal crash tubes.

Two initial *vehicle velocities* were examined: 25km/h and 40km/h. They represent a low velocity impact that is just below the lowest speed limit in most European countries and a high velocity impact that is the basis for the proposed draft directive [EEVC, 1998].

In terms of the *vehicle boundary conditions* the motion of the rigid rear end structure was limited to one degree of freedom in X and controlled by an imposed velocity curve to simulate 1g braking. Only an instantaneous initial velocity was applied to the remaining vehicle structure to match the initial velocity of the rear end. 1g braking deceleration was considered to be the maximum achievable with most modern vehicles and brake dive of 70mm typical for the front bumper of the C class vehicle examined. Finally, a global acceleration in Z was used to simulate gravity. An overview of the boundary conditions and global co-ordinate system is shown in Figure 17.

The *type of vehicle* was selected as a common car model of the total population and the type of pedestrian humanoid as the most validated model. A *pedestrian stance* of both legs together and side on to the vehicle was selected as a base case for future modelling comparisons.

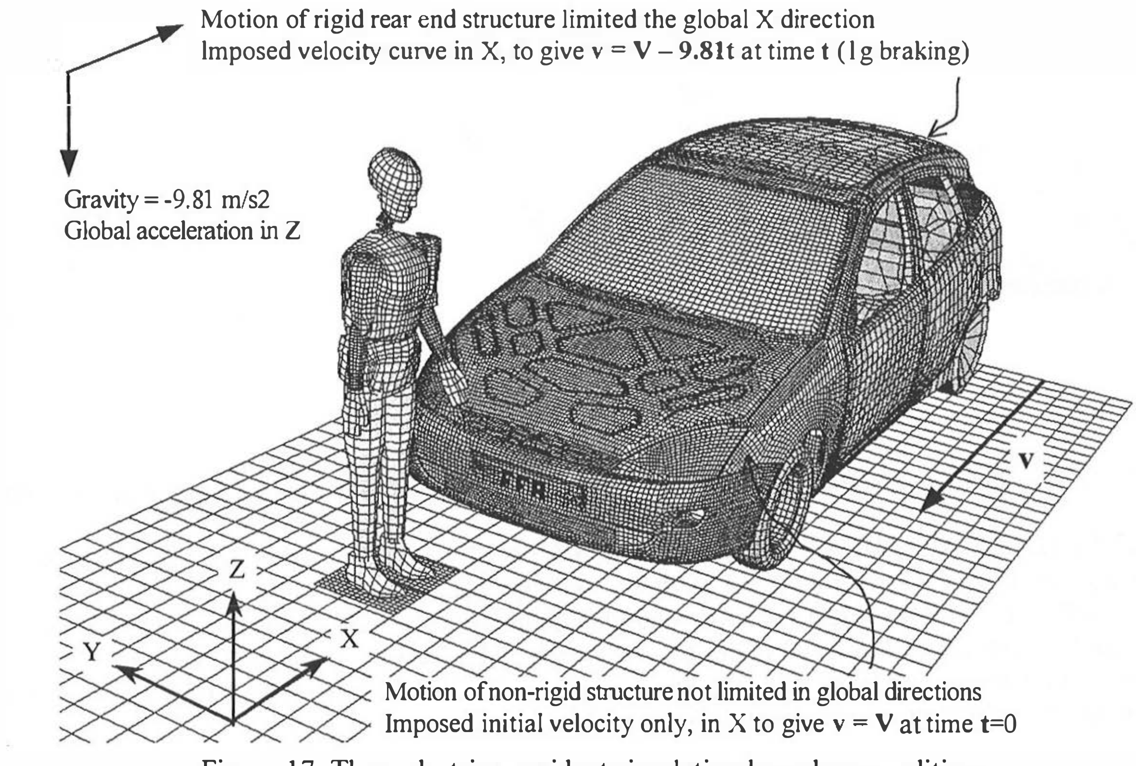

Figure 17 The pedestrian accident simulation boundary conditions

In this initial study, the subject of interest was the general behaviour of the simulation models over a relatively long solving time of 0.5 second. In order to limit the size of output files the simulations were limited to only produce output plots every 50ms.

RESULTS Figure 18 shows an example of one of the pedestrian accident simulations and the main impact events during an Y500 impact with a 40km/h initial vehicle velocity, brake dive and deceleration. Three main impact events were identified: full leg contact, pelvis/abdomen/arm contact and finally head contact as shown in frames 1, 2 and 4.

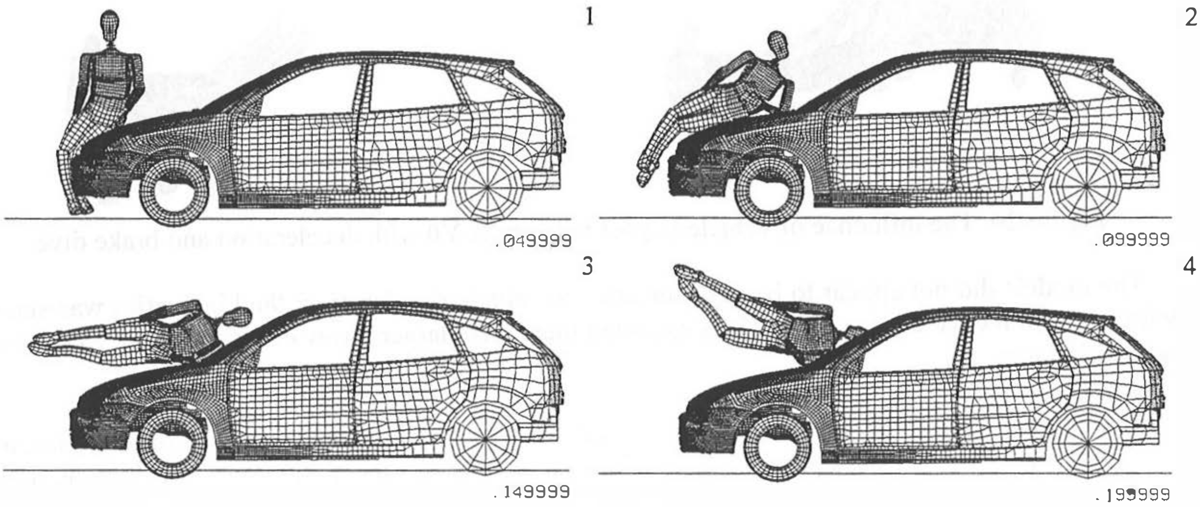

Figure 18 Y500 accident simulation with initial 40km/h vehicle velocity, brake dive and deceleration

The timing of the three main impact events for the twelve simulation runs may be summarised by grouping together the results by velocity as shown in Table 6.

	Range of times (ms) to		
Velocity (km/h)	Full leg contact	Pelvis/abdomen/arm contact	Head contact
25	10 to 50	150 to 200	250 to 350
40	10 to 50	100 to 150	150 to 200

Table 6 The timing range of the main pedestrian accident impacts for all boundary conditions

In all twelve simulations listed in Table 5 the throw distance in the X-axis (i.e. the absolute distance in the global X direction from the initial pedestrian standing position) is significantly greater than the lateral motion in the Y-axis.

At the Y500 impact location the humanoid model has a more pronounced rotation about the Z-axis than at Y0 as shown in Figure 19. However, at the Y0 impact location the throw distance in the X-axis is greater.

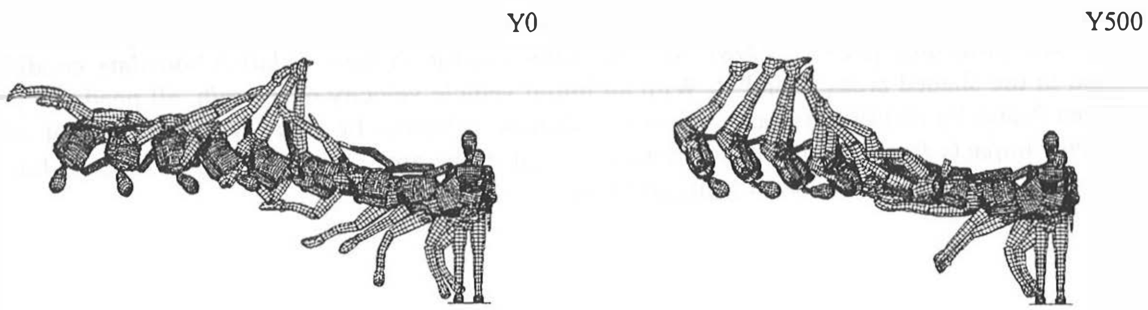

Figure 19 The influence of vehicle impact position at 40km/h with no deceleration or brake dive

As can be seen in Figure 20 the higher impact velocity leads to longer throw distances in the X-axis and Z-axis. Again, very little motion occurs in the Y-axis but there is a marked increase in rotation of the pedestrian about the Y-axis. In general, the higher impact velocity also exaggerates the influence of other accident boundary conditions such as vehicle deceleration.

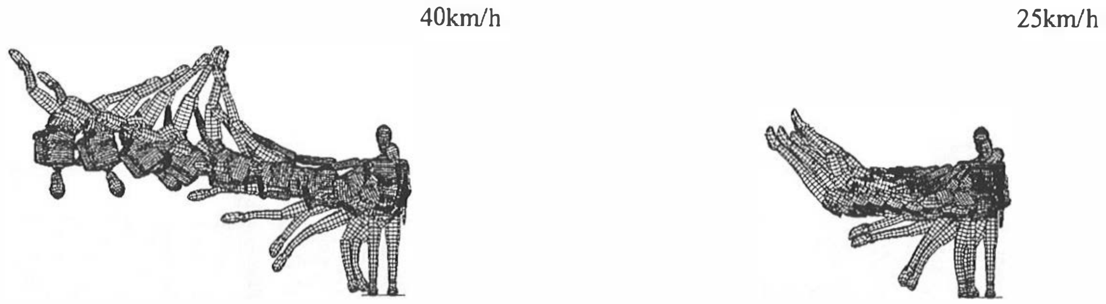

Figure 20 The influence of vehicle impact velocity at Y0 with deceleration and brake dive

The models did not appear to be very sensitive to *vehicle deceleration*; the kinematics was similar with or without deceleration although as expected there were larger throw distances in the X-axis with no deceleration.

In contrast to vehicle deceleration, *vehicle brake dive* had a very large influence on the humanoid kinematics, in particular at the higher vehicle impact velocity and the Y500 impact position as shown in Figure 21. Brake dive led to less rotation of the pedestrian about the Z-axis and longer throw distances.

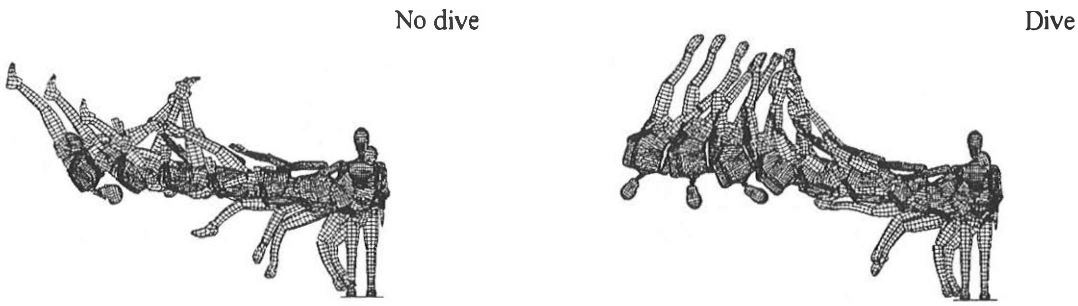

Figure 21 The influence of brake dive at Y500 with a 40km/h vehicle velocity and deceleration

In addition to general kinematics trends the pedestrian humanoid allows one to analyse specific model attributes. One of these is the relative velocity of the centre of gravity of the head to the vehicle and this can be related to each of the three main impact events listed in table 6 and identified in the general kinematics study, as shown in Figure 22.

This shows the range of relative head velocities for the range of simulation boundary conditions listed in Table 5. Relative head velocity is used because this can be related to the proposed draft directive test procedure [EEVC, 1998]. All head velocities for all the simulation boundary conditions occurred in the shaded areas A and B. With an initial vehicle velocity of 40km/h, all head velocities lie in area A and for an initial velocity of 25km/h all head velocities lie in area B. The timing of all the three main impacts for all of the simulations occurred in the areas 1 to 4. For example, all full leg contacts occurred in area 1 between 10ms and 50ms.

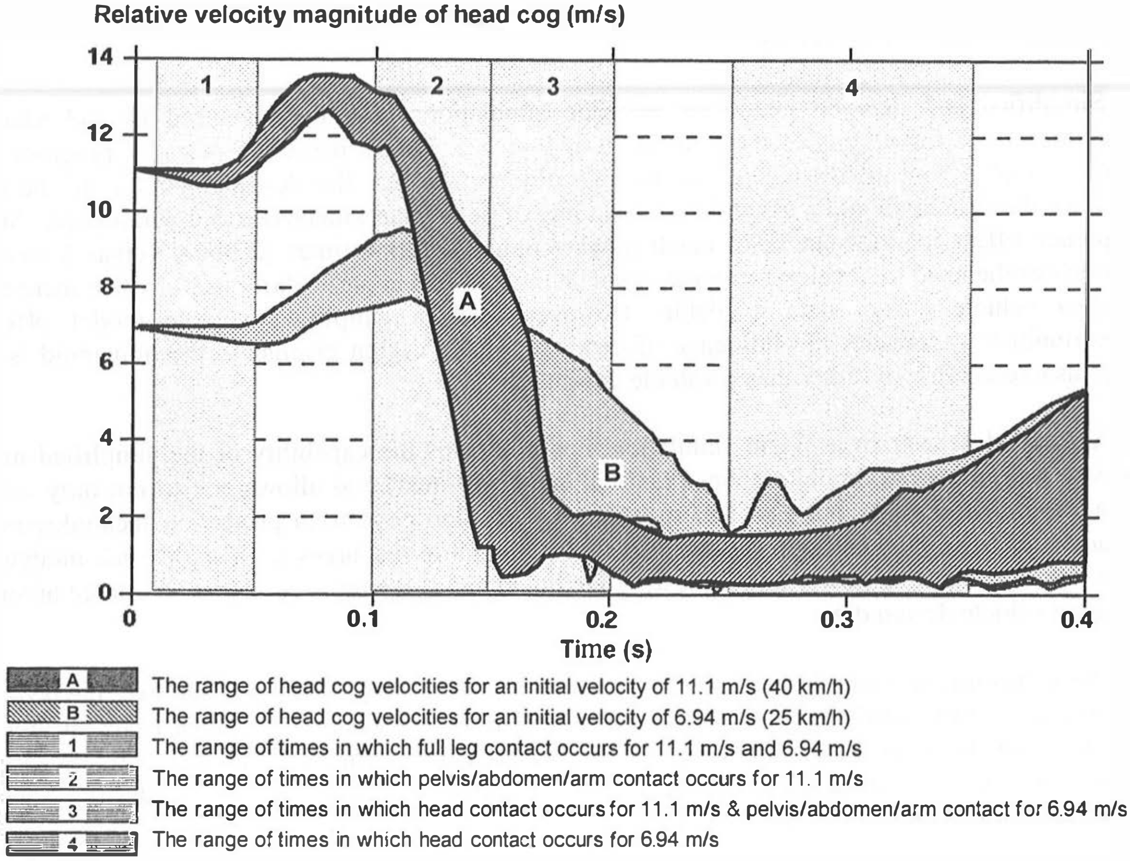

Figure 22 The range of head velocities relative to the vehicle for all simulation test matrix conditions

DISCUSSION It is to be expected that the throw distance in the X-axis is greater than any lateral motion in the Y-axis because the vehicle velocity is in the X-axis direction and the inertia of the vehicle is much greater than the pedestrian and hence the impact energy is primarily absorbed by the translational pedestrian motion in this direction.

When comparing the two impact locations the more pronounced rotation about the Z-axis at Y500 is caused by the vehicle front curvature in plan view. This rotational motion consumes some of the impact energy and leads to a shorter throw distance than at the Y0 location. This effect is reduced if brake dive is applied and/or the initial vehicle velocity is reduced to 25km/h. Clearly this is due to the lower impact energy which also explains the influence of two different velocities and the small difference caused by applying vehicle deceleration.

Vehicle brake dive caused the greatest difference in kinematics and particularly at Y500 and at the higher impact velocity. This supports other research studies [EEVC 1998] where a clear connection has been identified between the bumper height and the later kinematics. The bumper acts as a trip device that overcomes the foot to ground friction and sweeps the legs from under the pedestrian. If the bumper is lowered then there is a greater moment about the pedestrian centre of gravity and this leads to greater rotation about the Y-axis.

When one makes a comparison with the head impact test in the proposed draft directive, the areas of interest are associated with an initial vehicle velocity of 40km/h or more specifically the intersecting region of areas A and 3 in Figure 22. In this region all head impact velocities are significantly lower than the initial vehicle velocity. This is in contrast to the directive proposal, which specifies that the head impactors should be fired at the same velocity as the assumed initial vehicle velocity of 40km/h.

A COMPARISON BETWEEN THE SIMPLIFIED AND DETAILED PEDESTRIAN ACCIDENT SIMULATIONS

Simplified and detailed pedestrian accident simulations may be compared to understand the advantages and limitations of these different approaches. In this particular research program it was decided that a simplified vehicle structure should be used for the development of the humanoid models, the validation and a general understanding of pedestrian kinematics and parametrics. Such an approach offers the advantages of much quicker model solution times (2 hours versus 3 days) and eliminates the need to develop a complex vehicle model. This is particularly useful when there is very limited vehicle design data available. However, such a simplified vehicle model offers no opportunities to consider the influence of detailed vehicle design changes – the humanoid is being used as a research tool rather than a vehicle design tool.

A detailed pedestrian accident simulation model extends the capability of the simplified models, provides an improved model response (as will be shown next) and allows one to not only consider detailed design changes but also and subsequently develop pedestrian protection technologies. The disadvantages of such an approach are that it requires more resources to develop such models (e.g. man hours, computing power and rig testing facilities) and there must be access to a large amount of detailed vehicle design data.

One can compare many different model attributes, here the authors have chosen two: the pedestrian kinematics and the head centre of gravity velocity. The first attribute is the most basic attribute that the model needs to reproduce and the second the most sensitive to model differences. Figure 23 shows a comparison of pedestrian kinematics between simplified and detailed pedestrian accident simulations.

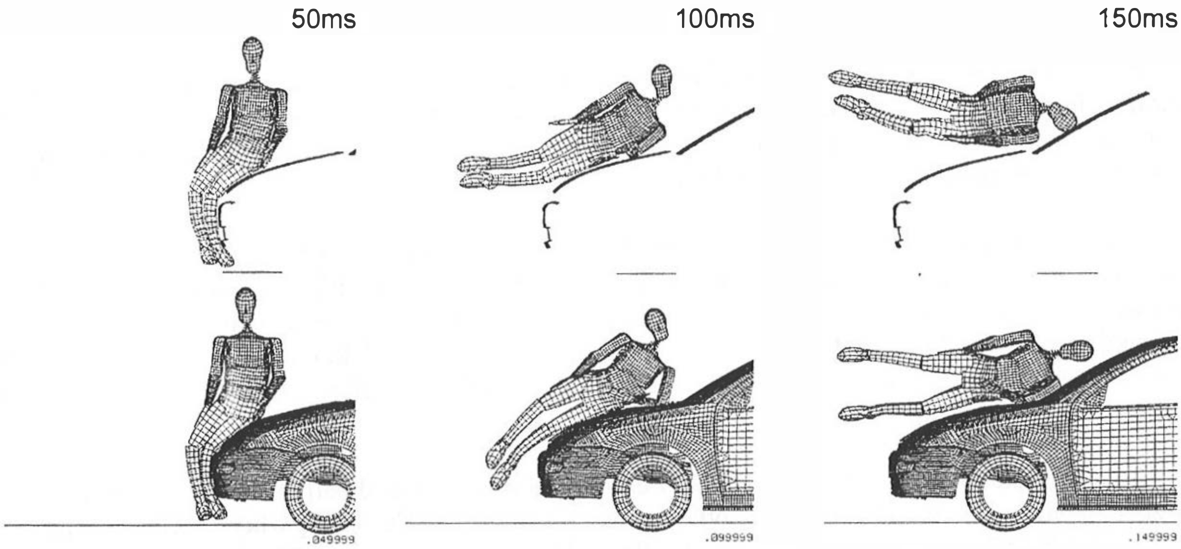

Figure 23 A comparison of pedestrian kinematics between simplified &detailed pedestrian accident simulations at Y0 with an initial 40km/h vehicle velocity, brake dive and deceleration

Up to 50 ms there are relatively minor differences between the humanoid kinematics. By 100ms, significant differences have developed, particularly in terms of the leg positions. The simplified model incorporates a rigid hood leading edge with a defined contact stiffness that is less able to absorb the impact energy. In turn this has led to greater rotation of the humanoid and in particular the humanoid legs about the Y-axis. There is also greater deformation of the humanoid upper leg. By 150ms the humanoid has been rotated even further and consequently the head impact has occurred more quickly in the simplified model. There has also been less energy absorbed through any arm contact and therefore one would expect a greater transfer of energy into the head contact.

If one now considers the global head velocity plot as shown in Figure 24 a number of differences are observed.

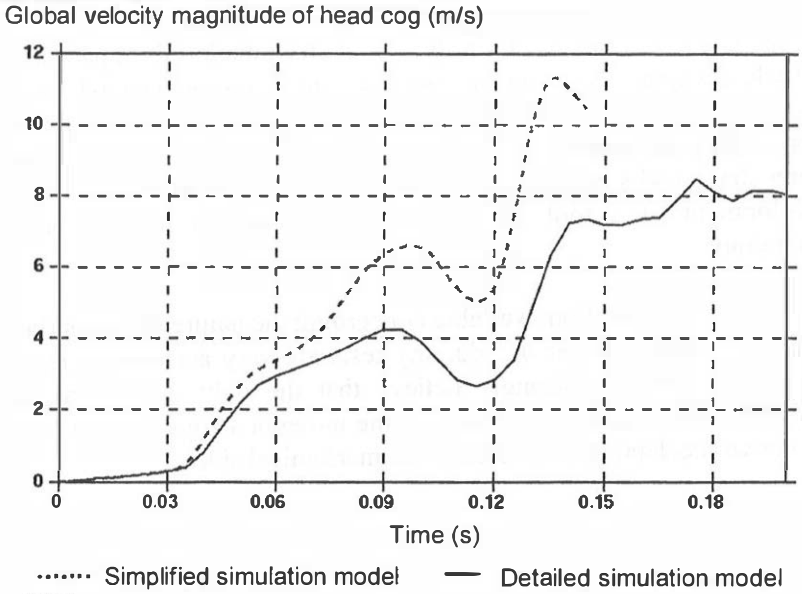

Figure 24 Pedestrian accident simulations at Y0 with an initial 40km/h vehicle velocity, brake dive and deceleration

Up to 144ms, which is the head impact event in the simplified model and the lower bound for the head impact events in the detailed model, the simplified model is predicting a higher head velocity. This is to be expected because the simplified vehicle absorbs less energy in the bumper system and subsequent hood impacts. Therefore, as shown in Figure 23, the pedestrian rotation is more rapid and consequently there are higher head velocities. Such a model is less able to predict head impact velocities.

CONCLUSIONS

The responses from the current humanoid formulation have been validated against staged cadaver tests by reference to kinematics/trajectories and measured parameters. It was clear that the validation could be improved further with more comprehensive cadaver limb size data. As the full flexible formulation of the humanoid is completed this exercise will be repeated to confirm its suitability and uniqueness as a vehicle design tool and real world accident reconstruction tool.

The initial development of pedestrian humanoid models and the use of one of these models in both simplified and more detailed pedestrian accident simulations have been described. It was demonstrated that both simplified and detailed pedestrian accident simulation models are useful in gaining a better understanding of the pedestrian and vehicle interaction. However, care should be taken when deciding which approach to take because they achieve different objectives. In essence, simplified pedestrian accident simulation models may be used as research tools whereas detailed pedestrian accident simulation models are vehicle design tools.

FUTURE RESEARCH

A major part of the future research program will clearly involve the further development and validation of the detailed real world pedestrian accident simulations because they provide the means to evaluate vehicle designs for real world pedestrian protection performance. The validation of such models will rely upon both the further enhancement of the pedestrian humanoids and access to much more detailed real world accident case studies. Both of these points are being addressed and both of these raise new issues to address.

For instance, when validation studies are conducted using information from cadaver tests or real-world accident reconstructions are conducted the overall height and weight of the subjects are insufficient data, instead individual limb sizes are needed to match the build of the subject to the geometry of the car. The development of a fully flexible formulation for a pedestrian substitute, or for that matter a vehicle occupant, is a vital necessity to aid in the understand and causation of injury mechanisms. Future work will develop this construction for a pedestrian (to include a segmented spine model representing all vertebrae). The ability to generate pedestrian models that reflect the diversity of human shape and size, adult and child, are an important element of pedestrian research. The further development of a tool for this purpose forms an integral part of the humanoid development programme.

There is also very little information available concerning the nature of pedestrian kinematics during real world accidents. Neither cadaver nor dummy tests are very accurate in reproducing real world behaviour. The authors therefore strongly believe that the only viable way to achieve a better understanding of pedestrian accident kinematics is the in-depth analysis of real world accidents, from both, the reconstructive-mechanical and medical-biomechanical sides.

REFERENCES

Akiyama, A., Yoshida, S., Matsuhasi, T., Rangarajan, N., Shams, T., Ishikawa, H. and Konosu, A. (1999), "Development of Simulation Model and Pedestrian Dummy", Advance in Safety Technology, SP-1433, SAE and International Congress and Exposition, paper 1999-01-0082, Detroit, Michigan, March 1999.

Ashton, S. J. (1978), Cause, "Nature and Severity of the Injuries Sustained by Pedestrians Struck by the Fronts of Cars or Light Goods Vehicles", PhD thesis, University of Birmingham, UK, 1978.

Bermond, F., Ramet, M., Bouquet, R., Cesari, D. (1993), "A Finite Element Model of The Pedestrian Knee-Joint in Lateral Impact", 1993 International IRCOBI Conference on The Biomechanics of Impacts", September 8-9-10th September 1993, Eindhoven (The Netherlands), pp 117-129.

Cheng, H., Obergefell, L. and Rizer, A. (1991), "Generator of Body (GEBOD) Manual", AL/CF-TR-1991-0051, Air Force Materiel Command, Wright-Patterson Air Force Base, Ohio.

EEVC/CEVE (1998), "Improved test methods to evaluate pedestrian protection afforded by passenger cars". Working Group 17 Report, December 1998.

Hardy, R.N., Watson, J.W., Howard, M.S (2000), "Developments in the Simulation of Real World Car to Pedestrian Accidents using a Pedestrian Humanoid Finite Element Model", International Journal of Crashworthiness, Vol 5 No 1, Woodhead Publishing Ltd, 2000.

Howard, M.S, Thomas, A.V, Philipps, M, Friesen, F (2000), "A Systematic Modelling and Testing Methodology to Characterise Vehicle Components under Pedestrian Impact Conditions", report to Ministerium für Wissenschaft und Forschung des Landes Nordrhein-Westfalen, February 2000.

Howard, M. S., Thomas, A. (1999), "An Integrated Approach to Real World Pedestrian Safety Research", Aachener Kolloquium Fahrzeug und Motorentechnik, Aachen, October 1999.

Howard, M.S., Thomas, A. (1998-1), "Pedestrian Safety Research - Past, Present, Future", Euromotor Tagung Crashworthiness - Crash Tests - Simulations, Institut für Kraftfahrwesen Aachen, Aachen, December 1998.

Howard, M.S., Watson, J.W., Hardy, R.N. (1998-2), "The Simulation of Real World Car to Pedestrian Accidents using a Pedestrian Humanoid Finite Element Model", International Journal of Crashworthiness, Vol 3 No 4, Woodhead Publishing Ltd, 1998.

Ishikawa, H., Kajzer, J. and Schroeder, G. (1993), "Computer Simulation of Impact Response of the Human Body in Car-Pedestrian Accidents", 37th Stapp Car Crash Conference, San Antonio, Texas, November 1993.

Jager, M.K.J. de (1996), "Mathematical Head-Neck Models for Acceleration Impacts", PhD thesis, University of Eindhoven, Netherlands, 1996.

Langwieder, K., Danner, M., Wachter, W. and Hummel, T. (1980), "Patterns of Multi-Traumatisation in Pedestrian Accidents in Relation to Injury Combinations and Car Shape", Proceedings of Eighth International Technical Conference on Experimental Safely Vehicle, Wolfsburg, Germany, October 1980.

MacLaughlin, T.F., Hoyt, T.A. and Chu, S.M. (1987), "NHTSA's Advanced Pedestrian Protection Program", 11th International Technical Conference on Experimental Safety Vehicles, 1987, SAE Paper 876100.

Organisation for Economic Co-Operation and Development (OECD) (1998-1), International Road Traffic and Accident Database (IRTAD). Note: EU data from 1979-1983 includes the Portugal pedestrian fatality number of the year 1984 and the 1997 as well as 1996 contains 1995 data from Greece and Portugal. Fatal means 30 day period, except Italy (7 days), France (6 days), Spain before 1993 (24 hours), Greece before 1996 (3 days), Austria until 1991 (3 days), Swiss before 1992 (unlimited), Japan before 1993 (24 hours), Portugal (24 hours). For these countries and time periods correction factors are used. The countries and regions are chosen according to their economic importance and the availability of reliable, consistent data.

Organisation for Economic Co-Operation and Development (OECD) (1998-2), International Road Traffic and Accident Database (IRTAD),. Note: 1995 data used except the EU figure which includes Italian and Luxembourg data from 1994.

Philipps M., Howard M.S. (1999), "FEA-Simulation of Vehicle - Pedestrian Collisions", ATZ Automobiltechnische Zeitschrift, August 1999.

Suthurst, G.D. and Hardy, R.N. (1985), "Computer Simulations of a Range of Car-Pedestrian Collisions", Proceedings of 10th International Technical Conference on Experimental Safety Vehicles, Oxford, England, 1985.

Yoshida, S., Matsuhashi, T. and Matsuoka, Y. (1998), "Simulation of Car-Pedestrian Accident for Evaluate Car Structure", Proceedings of 16th International Technical Conference on the Enhanced Safety of Vehicles, Windsor, Canada, June 1998.